Micro-device's Susceptibility Difference Based MRI Positioning System, a Preliminary Investigation

O. Felfoul[1], S. Martel[1], G. Beaudoin[2], J-B. Mathieu[1]
[1]NanoRobotics Laboratory, Department of Computer Engineering and Institute of Biomedical Engineering, École Polytechnique de Montréal (EPM), Campus of the Université de Montréal, Montréal (Québec) Canada
[2]Radiology Department, Faculty of Medicine, Université de Montréal, Canada

ouajdi.felfoul@polymtl.ca at www.nano.polymtl.ca

Abstract—**A positioning technique for an endovascular microdevice propelled by magnetic force inside a Magnetic Resonance Imaging (MRI) system is being developed. Positioning options are presented and a magnetic positioning technique is described in more details. Since a magnetic positioning system is deeply dependent on the quality of the measurement modality, we describe the main magnetic field measurement techniques that can be used inside an MRI. Finally, we propose a magnetic positioning system using MRI phase images to measure the magnetic distortion induced by the ferromagnetic body. Positioning results on a 1010/1020 carbon steel, 1.5875 mm diameter sphere with gradient echo phase images are presented.**

Keywords—**Field mapping, micro-device, MRI, phase images, positioning, sensors**

I. Introduction

Minimally invasive surgery allows surgeons to dramatically reduce patient discomfort and recovery time. However, the minimum size and curvature radius of the catheters prevents an extensive access to the cardiovascular system. Thanks to the advances in microfabrication techniques, the design of untethered microdevices able to explore the most remote areas of the cardiovascular system is becoming possible. The MR-Sub project (Magnetic-Resonance Submarine) is one of our first steps toward that goal. It relies on using an external magnetic field as a means of propulsion to bypass the problems linked to a bulky, difficult to miniaturize, and prone to failure active propulsion system.

A ferromagnetic core embedded in the micro-device will provide the driving force from an MRI system [1]-[2]. Real-time positioning of the MR-Sub is of primary importance since a flaw in the tracking system might have catastrophic consequences on the patient's health. As described in numerous studies, ferromagnetic materials have a very strong effect on images produced with MRI systems [3]-[4]. They induce non-linear distortions on the position and intensity of the pixels, which cause very large image artifacts. Moreover, the size of the distortions can be several times larger than the size of the ferromagnetic bodies that created them. These artifacts would prevent the use of conventional amplitude MR images for the positioning of the MR-Sub. Ferromagnetic distortions in the MRI field can be seen as much as a problem than as an asset. As a matter of fact, the magnetization of the MR-Sub can be used as an indication of its presence. Based on this principle, alternative solutions are being developed in our laboratory. They are described in the following sections.

II. Positioning Options

The difficulty in positioning is due to the small dimensions of the device and the complex environment in which it operates. Proposed dimensions of the device will be about 1/3 the vessel diameter for adequate trade-off between magnetic and drag force. In fact, the human body is a very complex and a very heterogeneous medium. Additional constraints come from the MRI magnetic environment, RF pulses and gradients on/off switching. Any external instrument added in the MRI environment must be magnetically compatible [5]. Caution must be taken to eliminate any risks on the health of the patients.

Imaging Modalities

Unfortunately, image artifacts prevent the use of an MRI system to directly track the position of the micro-device. Even if magnetic susceptibility artifacts have been well studied, there is currently to our knowledge no general method to correct for these distortions. Tracking with MRI images implies modeling the artifact and generating a map of a human body before insertion of the device. A method less dependent on the image artifact using the MRI facilities is described later in this paper.

Other imaging modalities have been investigated, among them ultrasound and fluoroscopy. Resolution of new ultrasound aperture can be high and is function of the wavelength used. Reducing the wavelength increases the resolution but at the same time, it decreases the penetration hence, the Field-Of-View (FOV). In order to position a moving device, a power Doppler ultrasound can be used. Signal from the device can be easily discriminated from the blood flow signal. Unfortunately, although ultrasonic MRI-compatible probe exist and are mainly used in minimally invasive surgery and biopsy needle guidance, the use of ultrasound increases the heat in the region of interest.

X-ray imaging would definitely provide a very good spatial and temporal resolution. 3D positioning can be done with two fluoroscopic imaging chains oriented orthogonally. Of course this technique is invasive and extended exposure time can be harmful to the patient. However, to this day, there are no MRI compatible X-ray systems.

Magnetic Tracking

Magnetic tracking of the position of the micro-device is an interesting option since the ferromagnetic material induces a strong magnetic field that perturbs the MRI field. Unlike other types of wireless transmission waves, the magnetic field is not attenuated nor perturbed by the human body.

A unique solution for the position of a moving dipole can be found if the gradient tensor and the gradient rate tensor at the same point are known [6]. Depending on the magnetic sensing modalities, hardware or software implementation of a gradiometer can be used to measure the gradient tensor instead of the magnetic field. The SNR is increased by measuring a gradient since the major sources of noise have a weak fluctuation in space and will be negligible.

Choice of the sensors used for the purpose of positioning is the major concern, since resolution will depend greatly on the measurement quality. The magnetic field of a dipole decreases at a rate proportional to $1/r^3$, where r is the distance from the source. Hence, a small magnetized sphere will have a very weak contribution to the static magnetic field of the MRI at some distance. Among existing magnetic sensors, search coils, SQUID, Hall sensors or Nuclear Magnetic Resonance (NMR) magnetometers are all candidates for this application.

Search coils can be designed to measure weak fields but will only make the AC component available. It would only be possible to track the position of the device when it is in motion. Thus, positioning will be relative to the position at the origin and errors will be summated continuously.

The approach using SQUID magnetometers is the most sensitive magnetic measurement technique available nowadays. They rely on the superconducting properties of materials and on the Josephson Effect phenomena to measure extremely small variations in magnetic flux. This magnetometer is used in biomedical application to monitor the magnetic field from the brain whose magnitude can be as weak as 10^{-14} T. However many technical difficulties arise when designing such a system. In fact, the SQUID sensor and the sensing coil must be maintained at a temperature below their superconducting transition temperature in a special container known as a dewar. The sensing coil may operate in the very high field of an MRI system, but the SQUID sensor must be maintained at a maximum magnetic field of 10mT and must be outside of the MRI bore. Still, the two components must be cooled and a special dewar must be designed for this application. Design of such a system must be very stable and any vibration can lead to errors in measurement. The SQUID system must be compact to fit inside the relatively narrow bore of most MR systems, and it must be easily moved in and out of the MR scanner. The high price of the SQUID is another limiting factor.

Hall sensor can be used only for medical applications near the surface of the skin due to their poor resolution that is about 10^{-4} T. We have used these sensors for in vitro positioning and algorithm validation as well as for propulsion and force characterization. Since the field in the z-direction is very strong, it does not allow measurement of the weak field in any other direction. Therefore, only one component of the magnetic field can be measured (z-component).

Finally, MRI can be used to map a magnetic field with phase images. These data allow gradient estimation of the magnetic perturbation due to the dipole's magnetic field. This technique can have a very good spatial resolution but a poor temporal one. As a matter of fact, use of MRI as a magnetic field mapping system for positioning purpose must be done at the same time as propulsion and an efficient multiplexing time algorithm has to be developed.

II. Theory

MRI Magnetic Field

Magnetic field inside an MRI can be considered homogenous and static over a large volume. The spatial encoding of the MRI images uses three spatial gradients that are switched on/off during sequence time. Finally, excitation of the spins is achieved with a short duration RF field. The presence of a human body inside the MRI bore induces perturbation to the static magnetic field due to the difference in susceptibility between air and the different human tissues.

Induced Magnetic Field

The ferromagnetic device will induce a magnetic field that is added to the main static field B_0 of the imager. The induced magnetic field exhibits an analytical formulation for simple shapes as a sphere but is generally modeled by a finite element analysis for complex geometries [4].

The induced magnetic field vector B' (T) of a sphere has the same form as a dipole with magnetization M (A/m) located at the origin and is described as

$$\vec{B}' = \frac{\mu_0}{3} a^3 \left[\frac{3\left(\vec{M}.\vec{r}\right)\vec{r}}{r^5} - \frac{\vec{M}}{r^3} \right], \qquad (1)$$

where $\mu_0 = 4\pi.10^{-7}$ H.m^{-1} is the vacuum permeability, r is the distance from the dipole and a is the radius of the sphere. The vector magnetization M is given by

$$\vec{M} = \frac{\chi_m}{\mu_0} \vec{B}_0, \qquad (2)$$

where χ_m is the susceptibility of the sphere.

III. Magnetic Field Measurement

In the previous sections, we have introduced many common techniques to measure magnetic fields. Here, we shall discuss the use of MR phase images to evaluate the induced magnetic field. Then, we shall investigate the possibility of using MRI as a magnetometer/gradiometer system to localize a magnetic dipole. The magnetic field mapping of dipolar source exhibits a characteristic shape that might be used to find the position of a ferromagnetic device in an MRI system.

MRI Phase Images

Phase imaging sequences generate a map of the magnetic field of the MRI system. They show the magnetic field inside the imaged volume rather than its biological structure. Phase images of a ferromagnetic sphere were taken. A gradient echo mapping sequence was run on a 1.5T Siemens Sonata MRI system with the following parameters: TE_1 = 10 ms, TE_2 = 14.76 ms, TR = 1000 ms, slice thickness = 5 mm. Images were taken in the coronal plane. In order to run a mapping sequence, an aqueous volume was used. It provides hydrogen protons and thus MR signal to the MRI machine. We placed a ferromagnetic sphere (1010/1020 carbon steel, 1.5875 mm diameter, saturation magnetization $1.33e^6$ A/m) in a cylindrical phantom of diameter = 180 mm filled with food gelatin (28 g/l). We added $NiSO_4.6H_2O$ (1.25 g/l) to decrease the relaxation time T1 and thus reduce the acquisition time of the images. The mapping sequence shows the field induced by the ferromagnetic dipole. A signal loss can be seen at the center of the dipole in Fig.1a and corresponds to voxels that did not contribute to the signal. This signal loss can be caused by the rapid spatial variation of the magnetic field near the sphere. In fact, a wrap in phase occurs every ~31μT of magnetic field variation as given by

$$\Delta\phi = \gamma B_z^{'} \Delta T_E \,, \qquad (3)$$

where γ is the gyro-magnetic factor for hydrogen having the value 42.58 MHz/T and ΔT_E used for the experiment is 4.76ms. The loss of signal can also be caused by the fact that the magnetic field near the sphere is very large, thus causing a shift in the resonance frequency of the protons in this area. Finally, the mathematical model describing the mapping in (3) uses only the perturbation along the z direction. But, near the sphere and, especially for ferromagnetic materials, the other two components (x and y) of the magnetic field can be important.

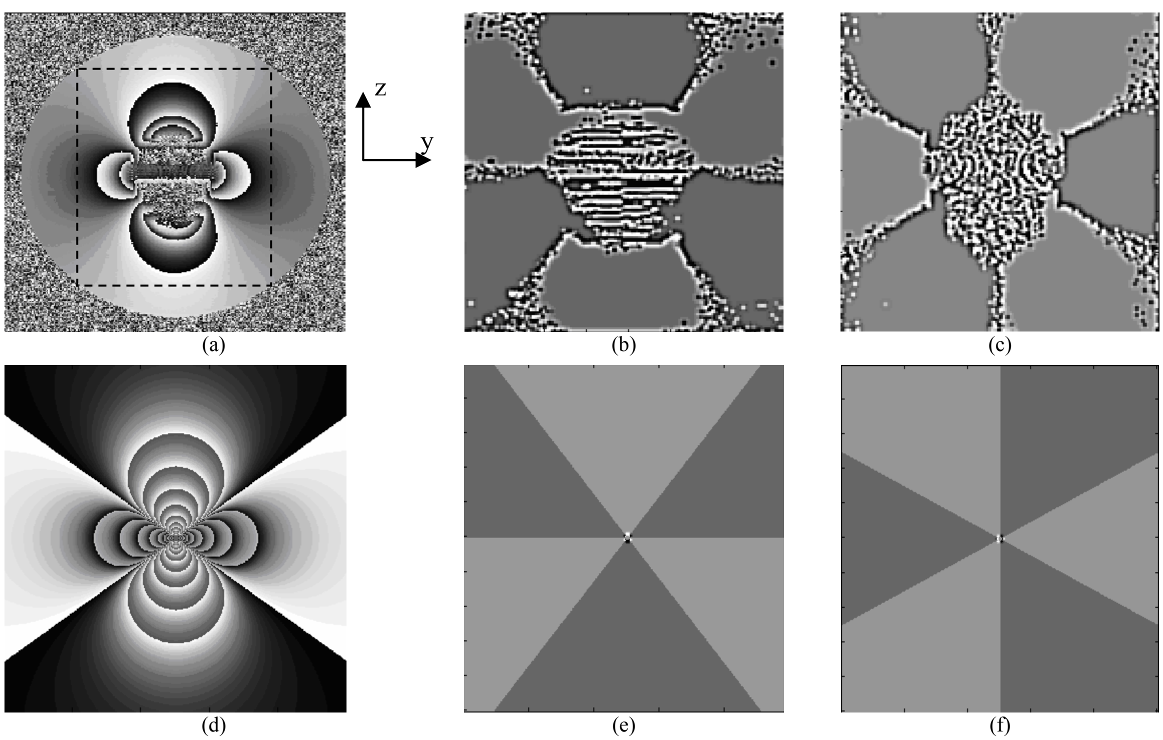

Fig.1. Magnetic dipole MRI phase image and gradient calculation; (a) Experimental field mapping of 1010/1020 carbon steel sphere, (b) Spatial gradient of experimental field mapping along the z direction, (c) Spatial gradient of experimental field mapping along the y direction, (d) Simulated field mapping of 1010/1020 carbon steel sphere, (e) Spatial gradient of simulated field mapping along the z direction, (f) spatial gradient of experimental field mapping along the y direction.

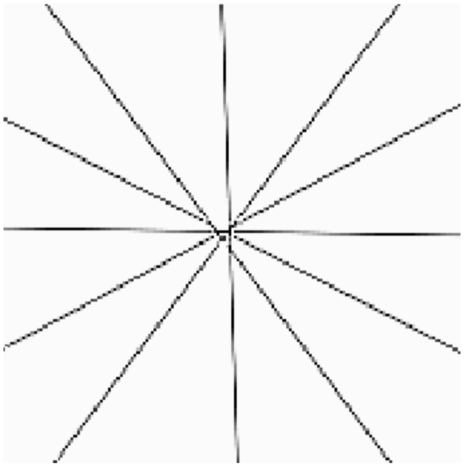

Fig. 2. Intersection lines of the change in sign of the magnetic gradient of the phase image. The convergence of the lines indicates the position of the dipole

IV. Positioning

We calculated the spatial gradient, Fig. 1 (b, c, e, f) to obtain more information on the dipole. Spatial gradient images are less contaminated than phase images by non-homogeneities of the magnetic field. As a matter of fact, the rate of change of the induced dipolar magnetic field is generally stronger than the one generated by any other perturbations. Therefore, these perturbations have less effect after derivation yielding an increase of the SNR.

As we are dealing with phase images, finding the absolute value of the magnetic field is very difficult due to lack of a reference point. In fact, the phase-dependent induced field is measurable even at the end of the phantom. Moreover, there is another induced magnetic field at the edges of the phantom due to the differences in susceptibility between air and the gelatin. To find the position of the dipole, we have found that it is much more appropriate to use the spatial gradients as in Fig. 1b and Fig. 1c. We calculated the gradient in the region delimited by dashed lines in Fig. 1a. Then, we have performed a Laplacian filter. Based on the theoretical model in Fig. 1e and Fig. 1f, the lines separating the regions where the gradient changes sign converges to the position of the dipole. Fig. 2 shows the convergence area of these lines in the experimental images Fig. 1b and Fig. 1c. It was obtained by performing a line detector using a Radon transform on the gradient images of the experimental setup.

V. Conclusion

This work is a preliminary study on positioning techniques for a ferromagnetic device propelled in a human body. Magnetic positioning techniques seem to be the best alternative since the MRI magnetic susceptibility artifacts prevents the use of MR amplitude images as a positioning modality. Phase image and spatial gradient representation of the induced field give information on the position of a dipole. The technique proposed in this paper could also be used for paramagnetic and diamagnetic materials since it is based on susceptibility difference. Moreover, even though these experiments have been done with a sphere, other geometries will have the same magnetic inductions than a dipole when small enough dimensions are used. Furthermore, MRI is a relatively slow imaging modality and a real time positioning system can't be achieved uniquely with phase images. A hybrid positioning system using external sensors for real time position tracking concurrently to MR images can bypass these limitations. Reference [7] reports high precision mapping of the magnetic field with a resolution as weak as 10^{-12} T. Thus, this technique could potentially be improved to achieve better positioning resolution. The next step in this study is to determine the repeatability and absolute precision of the positioning system through a specially developed calibration platform.

Acknowledgment

This work is supported by a strategic grant from the Natural Sciences and Engineering Research Council of Canada (NSERC) and in part by a Canada Research Chair (CRC) in Conception, Fabrication, and Validation of Micro/Nanosystems. We acknowledge the support of Hôpital Notre-Dame and Centre Hospitalier de l'Université de Montréal (CHUM) that provided the infrastructure to conduct MRI tests. We also wish to thank our collaborators, Gilles Soulez and L'Hocine Yahia.

References

[1] J.-B. Mathieu, S. Martel, L. Yahia, G. Soulez, and G. Beaudoin, "Preliminary investigation of the feasibility of magnetic propulsion for future microdevices in blood vessels," *BioMedical Materials and Engineering*, unpublished.

[2] J.-B. Mathieu, S. Martel, L. Yahia, G. Soulez, and G. Beaudoin, "MRI Systems as a mean of propulsion for a micro-device in Blood vessels," *IEEE Engineering in Medicine and Biology,* vol. 4, pp 3419-3422, Sep. 2003.

[3] J.-B. Mathieu, S. Martel, L. Yahia, G. Soulez, and G. Beaudoin, "Preliminary studies for using magnetic resonance imaging systems as a mean of propulsion for microrobots in blood vessels and evaluation of ferromagnetic artifacts," Canadian congress on electric and computer engineering, vol. 2, pp. 835-8, 2003.

[4] S. Balac, G. Caloz, G. Cathelineau, B. Chauvel, and J. D. de Certaines, "Integral method for numerical simulation of MRI artifacts induced by metallic implants," *Magnetic Resonance in Medicine*, vol. 45, no. 4, pp. 724-7, Apr, 2001.

[5] Schenck J.F., "The role of magnetic susceptibility in magnetic resonance imaging: Magnetic field compatibility of the first and second kinds," Med. Phys. vol.23, no. 6, pp. 815-850, June, 1996.

[6] W. M. Wynn, "Magnetic dipole localization with a gradiometer: Obtaining unique solution," *International Geoscience and Remote Sensing Symposium*, vol. 4, pp. 1483-1485, 1997.

[7] L. Li, J. S. Leigh, "High-precision mapping of the magnetic field utilizing the harmonic function mean value property" *Journal of magnetic resonance* vol.148, no. 2, pp.442-8 Feb, 2001.